

Dielectronic recombination measurements for the Li-like ions: B^{2+} , C^{3+} , N^{4+} , and O^{5+}

P. F. Dittner, S. Datz, P. D. Miller, and P. L. Pepmiller
Oak Ridge National Laboratory, Oak Ridge, Tennessee 37831-6377

C. M. Fou

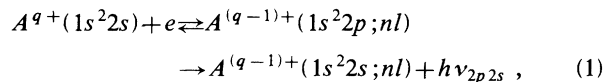
Department of Physics, University of Delaware, Newark, Delaware 19711

(Received 27 October 1986)

Dielectronic recombination rates via $2s$ - $2p$ excitation have been measured for the Li-like ions B^{2+} , C^{3+} , N^{4+} , and O^{5+} . We observe the amount of electron capture attending the passage of MeV/amu ion beams through a collinear, magnetically confined space-charge-limited electron beam as a function of relative energy. The measured rates show the predicted increase with Z but are higher than the rates calculated from the theoretically predicted cross sections. This is in contrast to the good agreement, between our measured rates and predictions from the same theory, found for Na-like ions.

I. INTRODUCTION

In an earlier paper¹ we reported on the measurements of dielectronic recombination (DR) for the Li-like ions B^{2+} and C^{3+} . Using a new technique which permits a reliable background subtraction, we have remeasured the DR for B^{2+} and C^{3+} and measured the DR for two more members of this isoelectronic series: N^{4+} and O^{5+} . The DR process measured for these ions is



where q equals the initial charge state of the ion, n and l are the quantum numbers of the captured electron, and ν_{2p2s} is the frequency of the emitted radiation of the core relaxation $2p$ to $2s$. We have described in detail our experimental apparatus, experimental procedure, and data reduction procedure in our previous paper² on DR measurements for Na-like ions, and only a brief description shall be given here. Finally, we shall compare the results for the Li-like ions with theory and with the results for the Na-like ions.

II. EXPERIMENTAL APPARATUS AND PROCEDURE

A merged-beam approach (the apparatus is outlined in Fig. 1) is used to take advantage of our ability to produce highly charged states, E/A (MeV) ions, and a high-current, high-energy electron beam. The ion beam from the Oak Ridge National Laboratory EN-tandem accelerator enters the interaction region through an axial hole in the cathode of the electron gun. In the interaction region, the ion beam is coaxial with and embedded within the electron beam for a distance of 84 cm. After exiting the interaction region, the ion beam is charge state analyzed using an electrostatic deflector. The initial charge-state beam (the charge is $q+$) is deflected into a Faraday cup connected to a current integrator and the output pulses

are counted by a scaler. Ions that have picked up an electron [the charge is $(q-1)+$] from the residual gas molecules, from slit-edge scattering, and from the sought after effect DR are deflected onto a solid-state position-sensitive detector (PSD). The pulses from the PSD are amplified and energy-gated position spectra are stored. The energy gating causes position pulses having an associated energy pulse less than 95% of the pulse height of the initial beam to be rejected, thus rejecting some of the pulses due to slit-edge-scattered ions.

The source of the electron beam is a high-intensity electron gun which produces a convergent, laminar electron beam. The emerging electron beam enters a coaxial solenoidal magnetic field which is adjusted to establish Brillouin flow.³ Surrounding the electron beam is a coaxial stainless-steel cylinder to which an electrical bias is applied. The application of an 11-Hz square-wave modulated voltage (having the values 0 and $+V_l$, alternately) to the cylinder allows us to modulate the electron velocity at a fixed cathode voltage V_c . Following the interaction region, defined by the length l , of the coaxial cylinder and the solenoidal field, the electron beam expands due to space-charge repulsion and strikes the chamber walls.

The relative energy (E_r) region in which DR can occur must be such that $0 \leq E_r \leq E_m$, where E_m equals the energy difference between the $2s$ and $2p$ level in the A^{q+} ion, 6.0, 8.0, 10.0, and 12.0 eV for B^{2+} , C^{3+} , N^{4+} , and O^{5+} , respectively. The relative or center-of-mass energy of an ion and a collinear electron is given by

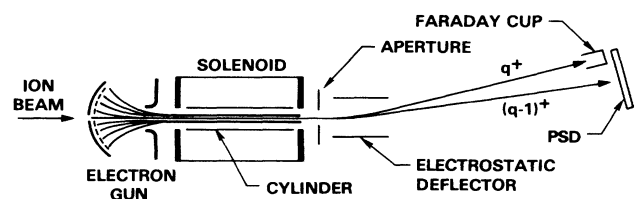


FIG. 1. Schematic view of the merged-beam apparatus.

$$E_r = \mu [E_e/m + E_i/M - 2(E_e E_i/mM)^{1/2}], \quad (2)$$

where μ is the reduced mass, m and E_e are the mass and energy of the electron, and M and E_i are the mass and energy of the ion, respectively. Because of the angular velocity of the electrons about the beam axis, collinearity can only be achieved on the ion (or electron) beam axis. Radial and angular misalignments of the two beams, angular divergence of the ion beam, and non-Brillouin flow electron beam behavior further invalidates the exact applicability of Eq. (2) in this experiment. However, these effects produce primarily a spread in E_r (see discussion below on the signal shape) and we will use Eq. (2) to give the centroid E_r .

We extract the DR signal from the recorded number of $A^{(q-1)+}$ ions per incident A^{q+} ions as we change E_r by changing E_i while keeping E_e (or V_c) fixed. The maximum ion energy E_{im} available from the EN tandem equals $6(q+1)$ MeV and this determines our choice of V_c such that $E_r=0$ for $E_i=E_{im}$, i.e., from Eq. (2), $E_e=(m/M)E_{im}$. This procedure maximizes V_c , which maximizes the electron density ρ_e , since $\rho_e \propto V_c$ for a space-charge-limited electron beam. This in turn maximizes the signal because the signal is proportional to ρ_e .

An 11-Hz square-wave voltage, alternating between 0 and $+V_t$ (referenced to ground), was applied to the cylinder surrounding the electron beam. V_t is chosen such that the resulting electron energy [$E_e=e(-V_c+V_t)$] together with E_i result in an E_r at least 5 eV above E_m , i.e., a region where no DR signal is expected. We count the $(q-1)+$ and $q+$ beams taking 1-eV steps in E_r by changing E_i . The number of ions when the cylinder voltage is zero, $N_0^{(q-1)+}$ and N_0^{q+} , or when the cylinder voltage equals $+V_t$, $N_v^{(q-1)+}$, and N_v^{q+} , are stored in separate channels. At each E_i we form the ratios

$$R_0 = N_0^{(q-1)+} / N_0^{q+} \quad \text{and} \quad R_v = N_v^{(q-1)+} / N_v^{q+}.$$

The result of such a procedure is shown for C^{3+} in Fig. 2, where we have plotted these two ratios versus E_r . Several jumps appear in the data which are much larger than the statistical error. These jumps probably occur because of slit-edge scattering which may vary somewhat with ion beam steering at different energies.

The ratio R_0 is composed of the signal R_s , plus the background R_b , whereas each R_v contains only background. Figure 3 is a plot of the difference ($R_0 - R_v$) versus E_r for the same C^{3+} run as in Fig. 2, and it can be seen that the jumps have disappeared. Small ($\sim 5\%$ of R_v) residues left after taking the above difference were subtracted as described in our earlier paper² and R_s determined versus E_r for all ions.

R_s is related to the DR cross section σ , by

$$R_s = \frac{\int \int \rho_i v_r \sigma(v_r) \rho_e dv_r d\Omega}{\int \rho_i v_i dA},$$

where ρ_e and ρ_i are the electron and ion density, respectively, and v_r and v_i are the relative and ion velocity, respectively. The area of integration in the denominator is the cross section of the ion beam and since ρ_i and v_i are

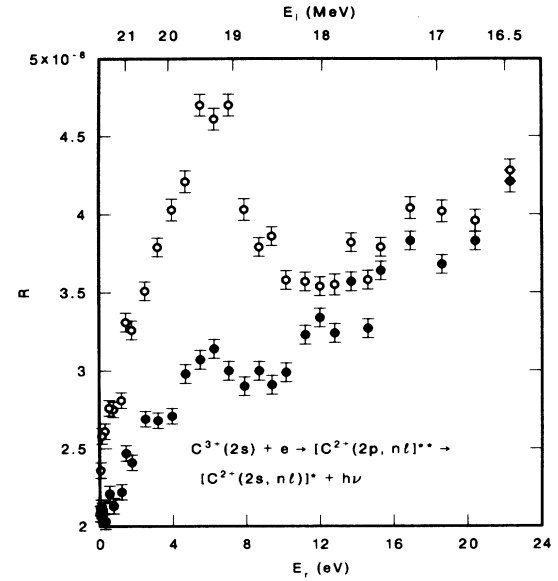


FIG. 2. The ratio's R_0 (\circ) and R_v (\bullet) vs E_r for C^{3+} . See text for definition of R_0 and R_v .

almost constant within the volume Ω , we can in good approximation write that $\int \rho_i v_i dA = \rho_i v_i A$. The volume of integration Ω in the numerator is defined by the area A , and the length of the electron beam L . Approximating ρ_e by an average electron density, $\bar{\rho}_e$ times a distribution in relative velocities $f(v_r)$, both being independent of position within Ω , we can write that

$$R_s = (\bar{\rho}_e L / v_i) \int v_r \sigma(v_r) f(v_r) dv_r = (\bar{\rho}_e L / v_i) \langle v_r \sigma \rangle.$$

Thus from the measured quantities we can calculate a quantity, $\langle v_r \sigma \rangle$, having the dimensions of a rate, at every E_i or E_r , i.e., $\langle v_r \sigma \rangle = R_s v_i / (\bar{\rho}_e L)$.

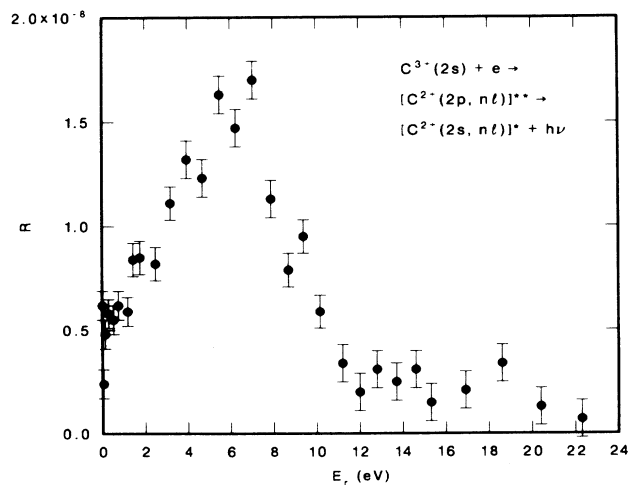


FIG. 3. The difference $R (= R_0 - R_v)$ vs E_r for C^{3+} .

III. THEORY-EXPERIMENT COMPARISON

In order to compare our results to calculations, we shall first review the properties of the DR cross section σ , and then discuss how our experiment affects the comparison with the theoretical predictions. The σ predicted to be observed under the conditions of this experiment depends on the electric fields present in two regions: first, the charge-state analysis region and second, the interaction region.

The electric field used for the charge-state analysis can field ionize states of the $A^{(q-1)+}(\alpha; n, l)$ having high n values. The maximum n that can survive these fields is approximately given by⁴

$$n_m^4 = 6.31 \times 10^8 q^3 E_a, \quad (3)$$

where q is the core charge and E_a is the analysis field in V/cm. In this experiment the deflection field used was ~ 4.5 kV/cm and for B^{2+} , C^{3+} , N^{4+} , and O^{5+} , $n_m = 32$, 44, 54, and 64, respectively. Hence, ions that have undergone DR but with $n > n_m$ will be field ionized and not be present in the $(q-1)+$ signal channel. Therefore, the DR rate extracted from the data will be only a fraction of the total DR which occurs in the interaction region.

The space charge of the electron beam causes a radial electric field in the interaction region E_{ir} , which can mix l states for a given n , and thereby increase the DR cross section. The effect of electric fields on the DR cross section has been considered by Griffin, Pindzola, and Bottcher⁵ for Li-like ions (B^{2+} , C^{3+} , and O^{5+}) and Na-like ions (P^{4+} , S^{5+} , and Cl^{6+}), and by LaGattuta⁶ for Li-like ions (B^{2+} and C^{3+}). Where they overlap, the two calculations give almost identical results. Figure 4 shows the results of a calculation⁵ for the O^{5+} DR cross section versus n ($n \leq n_m = 64$) for five values (0, 5, 25, 125, and 625 V/cm) of E_{ir} . The σ exhibits many sharp resonances versus energy (having widths $\ll 0.01$ Ry) but for convenience of

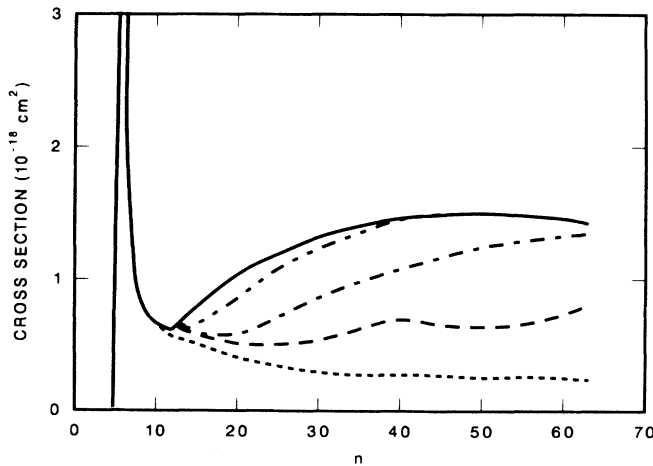


FIG. 4. The DR cross section for O^{5+} vs n (for $n_m = 64$). E_{ir} (in V/cm) = 0, \cdots ; 5, $---$; 25, $- \cdot - \cdot -$; 125, $- - - -$; 625 $---$.

presentation and comparison with experiment, it is useful to define $\bar{\sigma}$, averaged over an arbitrarily chosen energy interval Δe , as

$$\bar{\sigma}(E_r) = \frac{1}{\Delta e} \int_{E_r - \Delta e/2}^{E_r + \Delta e/2} \sigma de.$$

For $\Delta e = 0.01$ Ry which is much smaller than our experimental energy resolution but larger than the largest resonance width, $\bar{\sigma}$ carries the same information as σ itself. A logarithmic histogram of $\bar{\sigma}$ versus E_r for C^{3+} is shown in Fig. 5 for $\Delta e = 0.01$ Ry, $n_m = 44$, and $E_{ir} = 25$ V/cm.

We take the calculated⁵ $\bar{\sigma}$, multiply by v_r , and convolute with our relative velocity distribution $f(v_r)$ in order to get a calculated value for $\langle v_r \bar{\sigma} \rangle$. The procedure is repeated for each value of the field in the interaction region for which a $\bar{\sigma}$ is calculated yielding $\langle v_r \bar{\sigma} \rangle$ versus E_r for 0, 5, 25, 125, and 625 V/cm. The $f(v_r)$ is broken down into a transverse (with respect to the ion beam), f_{\perp} , and parallel, f_{\parallel} , component given by

$$f_{\perp} = 2\beta v_{\perp} \exp(-\beta^2 v_{\perp}^2),$$

and

$$f_{\parallel} = \alpha / \sqrt{\pi} \exp[-\alpha^2 (v_{\parallel} - v_0)^2],$$

where v_{\perp} and v_{\parallel} are the electron velocity components transverse and parallel to the ion beam, respectively, v_0 is given by

$$v_0 = (2E_r / m)^{1/2},$$

$\alpha = 6.89 \times 10^{-8}$ sec/cm, and $\beta = 7.55 \times 10^{-9}$ sec/cm. The values of α and β and the functional form of f_{\parallel} and f_{\perp} were deduced from our previous work² on Na-like ions.

The calculated $\langle v_r \bar{\sigma} \rangle$ for $E_{ir} = 0, 5, 25, 125$, and 625 V/cm and the data are shown in Figs. 6–9 for B^{2+} , C^{3+} , N^{4+} , and O^{5+} , respectively. The error bars indicated are the relative uncertainties, which include counting statistics and background subtraction. The absolute uncertainty is dominated by the imprecise knowledge of the electron density $\bar{\rho}_e$. We estimate the uncertainty in $\bar{\rho}_e$ to be

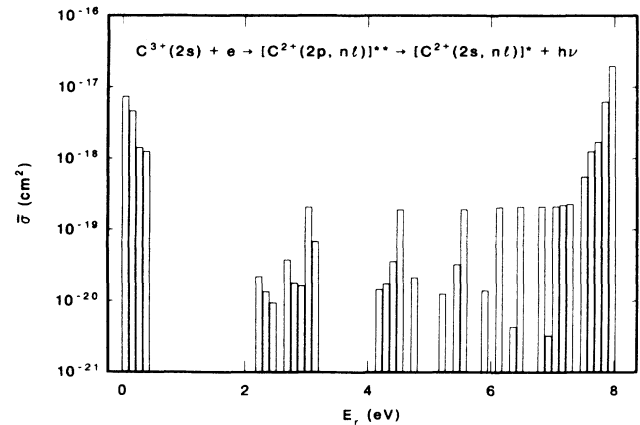


FIG. 5. The DR $\bar{\sigma}$ vs E_r for C^{3+} , $\Delta e = 0.01$ Ry, $n_m = 44$, and $E_{ir} = 25$ V/cm.

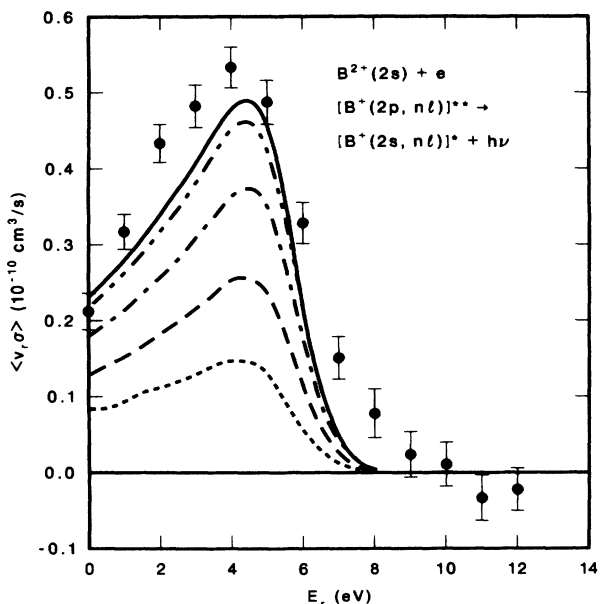


FIG. 6. The DR rate $\langle v_r \bar{\sigma} \rangle$ vs E_r for B^{2+} . The points are the experimental data, the curves are calculated from the $\bar{\sigma}$ of Ref. 5 for E_{ir} (in V/cm)=0, . . . ; 5, ---; 25, - · - · -; 125, - - - -; and 625, —.

$\pm 30\%$ and thus, the absolute uncertainty of the data is $\pm 35\%$. Two separate sets of data are shown in Fig. 7 for C^{3+} , in the first set $v_e > v_i$ (open circles) and in the second set $v_e < v_i$ (solid points). The agreement between the two sets of data is within statistical error and provides assurance that the signals seen depend only on v_r , as they

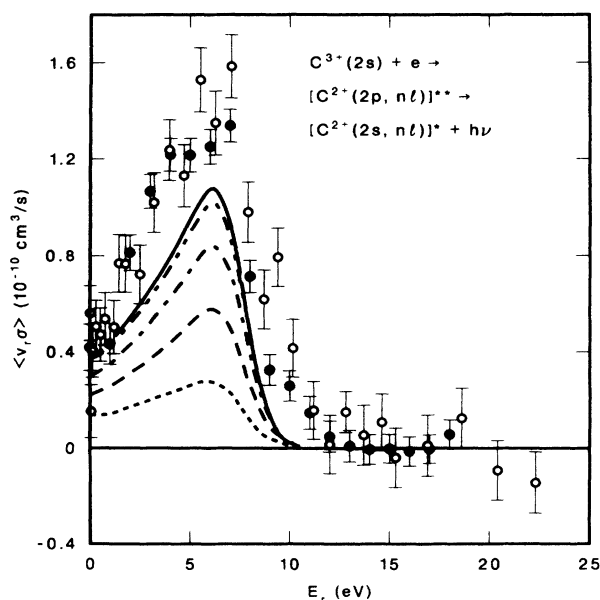


FIG. 7. The DR rate $\langle v_r \bar{\sigma} \rangle$ vs E_r for C^{3+} . Open circles are the experimental data for $v_e > v_i$ ($V_c = -1078$ V), solid circles for $v_e < v_i$ ($V_c = -840$ V), the curves are calculated from the $\bar{\sigma}$ of Ref. 5 for E_{ir} (in V/cm)=0, . . . ; 5, ---; 25, - · - · -; 125, - - - -; and 625, —.

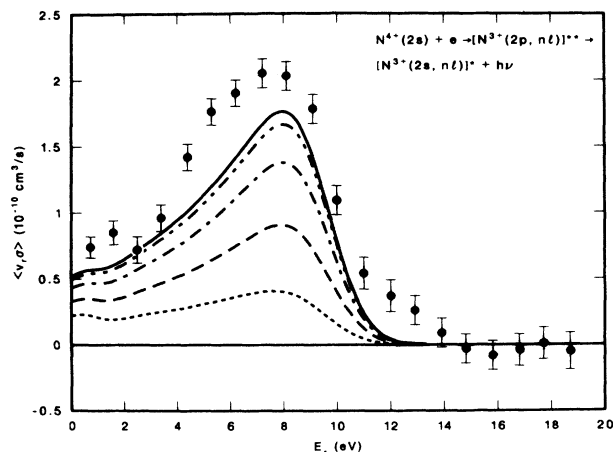


FIG. 8. The DR rate $\langle v_r \bar{\sigma} \rangle$ vs E_r for N^{4+} . The points are the experimental data, the curves are calculated from the $\bar{\sigma}$ of Ref. 5 for E_{ir} (in V/cm)=0, . . . ; 5, ---; 25, - · - · -; 125, - - - -; and 625, —.

should. Further evidence of this is shown in Fig. 9 for O^{5+} where again two sets of data are shown having different v_e 's, although here $v_e > v_i$ for both sets.

The actual E_{ir} of our experiment is difficult to assess precisely since it varies over the radius and length of the electron beam. If we assume that the electron beam is undergoing Brillouin flow, the electric field would range from 0 V/cm at the center ($r=0$ mm) to $0.2V_c$ V/cm at the outer edge ($r=1.58$ mm). Under ideal conditions, the

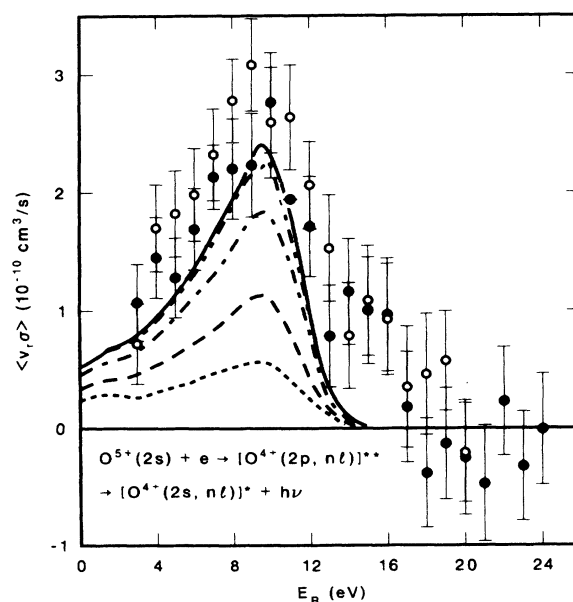


FIG. 9. The DR rate $\langle v_r \bar{\sigma} \rangle$ vs E_r for O^{5+} . The points are the experimental data for $V_c = -1414$ V (solid circles) and -1284 V (open circles), the curves are calculated from the $\bar{\sigma}$ of Ref. 5 for E_{ir} (in V/cm)=0, . . . ; 5, ---; 25, - · - · -; 125, - - - -; and 625, —.

ion beam is confined to a region ± 0.32 mm from the electron beam center and at $r = 0.32$ mm, E_{ir} reaches a value of $0.04 V_c$ V/cm. Thus, for a typical V_c of 1000 V, the field in the interaction region would have a maximum of 40 V/cm and an effective average field of 30 V/cm. However, if the axes of the two beams are slightly misaligned and/or scalloping of the electron beam occurs, mean values of E_{ir} can conceivably be twice as large. Values greater than this are not likely since the beams are aligned by minimizing the steering of the ion beam caused by the electron beam and since the electron energy distribution is an indicator for the amount of scalloping.

The data points, in order to agree with the theory, should fall between the calculated⁵ curves for 25 and 125 V/cm. As can be seen in Figs. 6–9 for all the Li-like ions, the experimental values exceed the theoretical values by approximately 60% if we assume ideal beam conditions or 30% if we assume a field twice as large. This is in sharp contrast to the agreement between our experimental results and the calculations (for $E_{ir} = 25$ V/cm) by the same authors for the Na-like ions as shown in Ref. 5. For the Na-like ions the cathode voltages used in our experiments and hence the fields in the interaction region were about half the values of the same quantities used in the experiments involving the Li-like ions.

We shall now consider whether l -changing collisions involving the recombined ion and an electron could enhance our measured DR rate. This process, first considered by Burgess and Summers,⁷ could increase the l of the intermediate state of Eq. (1) and decrease the autoionization rate back to the incoming state of Eq. (1) and in turn increase the DR rate. The fraction of ions affected, f , is given by

$$f = n_e \sigma_l x,$$

where n_e is the electron density and x is the distance traveled by the ion in the intermediate state, given by

$$x = v_i t = v_i A_a^{-1},$$

where A_a is the autoionization rate and σ_l shall be approximated by the geometric size of the Rydberg orbit, i.e.,

$$\sigma_l = \pi a_0^2 n^4 q^{-2},$$

where q is the charge state of the ion, n is the principal quantum number of the intermediate state, and a_0 is the Bohr radius. In our experiments, the maximum values of n to be considered are those which survive the analyzing field as given in Eq. (3) and listed above.

We will consider the case of O^{5+} as it was investigated in this work which should display the maximum effect. Here $V_c = -1414$ V (which maximizes n_e), $n = n_m = 64$ (which maximizes σ_l), and A_a equals approximately 1.5×10^{10} (which maximizes x), which gives the largest value of the fraction of ions which suffer an l -changing collision and is only 1.5%. The lower n states of this ion have an even lower f . For the other Li-like ions, lower

electron density beams were used, the n_m 's are lower, and larger A_a 's are calculated; all these effects should lead to an even lower fraction undergoing an l -changing collision. Furthermore, all l -changing collisions do not lead to higher values of l which increase DR and even some of those would still autoionize before stabilization, so the above is an overestimate. A variation in the electron density of approximately 30% in the C^{3+} experiment showed no change in the DR rate outside of statistical error bars of about 12%. Unfortunately, varying the electron density in our experiment by a factor of 2 could only be done by decreasing the electron density via a decrease in the cathode voltage and this in turn would force a decrease in the ion velocity. These factors would cause a serious decrease in the already poor signal to background ratio and therefore were not attempted.

In our DR measurements for the Na-like ions² the electron densities used were a factor of 2 lower than those used for our present measurements. However, the applicable n_m values are higher and the net result for l -changing events is similar to that obtained for the Li-like ions, e.g., for the case of Cl^{6+} of Ref. 2, $f = 1.2\%$. Thus, unless there is reason to believe that the σ_l for the Rydberg states of the Li-like ions is significantly different than that for the Rydberg states of the Na-like ions, the effect of l -changing collisions should be the same for the two different experiments.

Other measurements⁸ on Mg^+ (also Na-like) carried out at two different interaction region fields also exceed calculated values⁹ by 50% to 100%. Preliminary measurements¹⁰ of the DR cross section of C^{3+} using an inclined beams technique, with a known field of 10 V/cm in the interaction region and an electron density orders of magnitude lower than in our experiments, also give results which exceed the theoretical prediction by about a factor of 2. The measurements referred to above all involve $\Delta n = 0$ transitions where the cross section is dominated by capture to high n states and where field effects are important. Indirect measurements of DR σ 's via resonant transfer and excitation¹¹ of $\Delta n = 1$ transitions, where capture to low n states dominates and field effects are negligible, are in good agreement with theory.¹² Furthermore, it has recently been pointed out¹³ that the effect of the fields has been overestimated by the calculations performed to date, which if substantiated by specific calculations, would increase the discrepancy with experimental values for $\Delta n = 0$ transitions. At this point, it appears that further measurements of DR need to be carried out in order to resolve the disagreement with the theory.

ACKNOWLEDGMENTS

This research was sponsored by the U.S. Department of Energy, Division of Chemical Sciences, under Contract No. DE-AC05-84OR21400 with Martin Marietta Energy Systems, Inc. One of the authors (C.M.F.) acknowledges the support by Oak Ridge Associated Universities under Faculty Research Participation Contract No. S-3039.

- ¹P. F. Dittner, S. Datz, P. D. Miller, C. D. Moak, P. H. Stelson, C. Bottcher, W. B. Dress, G. D. Alton, N. Nesković, and C. M. Fou, *Phys. Rev. Lett.* **51**, 31 (1983).
- ²P. F. Dittner, S. Datz, P. D. Miller, P. L. Pepmiller, and C. M. Fou, *Phys. Rev. A* **33**, 124 (1986).
- ³P. T. Kirstein, G. S. Kino, and W. E. Waters, *Space Charge Flow* (McGraw-Hill, New York, 1965), p. 153.
- ⁴F. Broulliard, in *Atomic and Molecular Processes in Controlled Thermonuclear Fusion*, edited by C. J. Joachain and D. E. Post (Plenum, New York, 1983).
- ⁵D. C. Griffin, M. S. Pindzola, and C. Bottcher, *Phys. Rev. A* **33**, 3124 (1986).
- ⁶K. J. LaGattuta, *J. Phys. B* **18**, L467 (1985).
- ⁷A. Burgess and H. P. Summers, *Astrophys. J.* **157**, 1007 (1969).
- ⁸A. Müller, D. S. Belić, B. D. Paola, N. Djurić, G. H. Dunn, D. W. Mueller, and C. Timmer, *Phys. Rev. Lett.* **56**, 127 (1986).
- ⁹C. Bottcher, D. C. Griffin, and M. S. Pindzola, *Phys. Rev. A* **34**, 860 (1986).
- ¹⁰J. Kohl, L. Gardner, and A. R. Young, Proceedings of the Atomic Physics Program Contractors' Workshop (Program and Abstracts), Boulder, Colorado, 1986 (unpublished), pp. 63–65.
- ¹¹J. A. Tanis *et al.*, in *Atomic Excitation and Recombination in External Fields*, edited by M. H. Nayfeh and C. W. Clark (Gordon and Breach, New York, 1985).
- ¹²D. J. McLaughlin and Y. Hahn, *Phys. Lett.* **88A**, 394 (1982); I. Nasser and Y. Hahn, *J. Quant. Spectrosc. Radiat. Transfer* **29**, 1 (1983).
- ¹³D. A. Harmin, *Phys. Rev. Lett.* **57**, 1570 (1986).